CHAPTER 55

IRREGULAR WAVES OVER AN ELLIPTIC SHOAL

Xiping Yu[1] *and* Hiroyoshi Togashi[2]

ABSTRACT

A numerical model for the transformation of narrow-banded irregular waves over gradually varying bottom topography is presented. The model is based on the mild slope wave equation for component waves. Perturbation of the mild slope wave equation with respect to the deviation of the angular frequency of any component wave from that of a principal wave, which is a small quantity for waves of narrow-banded spectra, is carried out. The mild slope wave equation, which depends on the frequency of the component wave, can thus be replaced by the perturbation equations in terms of the principal wave parameters. The finite element method is considered for numerical solutions of the perturbation equations. Since the matrix of the linear algebraic finite element equations depends on neither the component wave properties nor the order of the perturbation, numerical solution of an irregular wave field can be efficiently obtained. The model is applied to the computation of the wave motion over an elliptic shoal. The computed wave height distribution shows satisfactory agreement with the available experimental data.

INTRODUCTION

The mild slope wave equation (Berkhoff, 1972) has been established as an effective model for describing the combined refraction and diffraction of small amplitude waves in nearshore zone. In spite of its widely recognized validity,

[1]Assoc. Prof., Dept. Civ. Eng., Nagasaki Univ., Bunkyo-Machi 1-14, Nagasaki City, Nagasaki 852, Japan

[2]Prof., ditto

application of this model in practice has, however, not always been easy. One of the reasons is the considerable computational efforts necessitated to solve the elliptic partial differential equation if the domain of interest has a dimension of over several wavelengths. The situation becomes even more critical if the wave irregularity is assumed to be of primary importance and, therefore, a large number of component waves must be dealt with independently. The research efforts on developing effective numerical methods so that the mild slope wave equation can be applied to the problems with large domain have led to many distinguishable achievements in the past decade. On improving the approach to the wave irregularity, however, less progress has been made.

Real sea waves are always irregular. However, most engineering analyses of the nearshore wave motion had long been based on representation of the real sea by monochromatic waves, usually the significant waves. The inaccuracy of such representation has been pointed out by many researchers who compared the results by the representative wave method with those by other more accurate methods (see, *e.g.*, Goda, 1985). Since the wave transformation processes are always frequency dependent, it can not be expected that the significant wave parameters of an irregular wave field are even close to the wave parameters following the transformation of the significant wave. This is particularly true in a region where waves undergo significant refraction and diffraction.

The most direct approach to the wave irregularity may be the superposition method. This classical method is based on decomposing irregular waves into monochromatic components with different frequencies. By applying a regular wave theory to each of these component waves and reassembling the solutions, the irregular wave field can be computed. As long as the wave is of small amplitude, or, is linear, the superposition method is authoritative. However, a large number of component waves must be considered to ensure the accuracy of results. Since the component waves are numerically independent, considerable computational efforts are necessary.

A rather different approach to the superposition is the energy method originally proposed by Karlsson (1969). This method is based on a governing equation in terms of the energy spectrum, which is generally expressed by the product of a wave height related parameter with a distribution function describing the spread of the wave energy with respect to the frequency and the directional angle. Once the distribution function is assumed to be invariant or to be in a known form in the domain of interest, the wave height can be accordingly solved from the governing energy equation. This method is direct but can not be widely applied because the spectrum is in fact part of the solution of an irregular wave field and it is not always appropriate to assume its invariance or foreseeability. In particular, if there is a permeable breakwater in the domain of interest, because of the frequency selectivity of the breakwater to reflection and transmission, the wave spectrum, at least, in the vicinity of the breakwater may undergo significant transformation. Any presumption on its form under this circumstance may lead to mistakes.

The present study is to provide a rather different approach to the irregular wave motion in nearshore zone. The method is essentially superposition but the computational effort involved is equivalent to that required by the representative wave method. In the following sections, we first describe the governing equation for the component wave and perturb the equation with respect to the deviation of the angular frequency of the component wave to that of the principal wave. Then, we illustrate the finite element method for solutions of the perturbation equations. Finally, we apply our numerical model to the wave motion over an elliptic shoal and compare the computational results with experimental data.

THEORY

The Basic Equation

For the component wave, with a small amplitude and an arbitrary angular frequency, over a gradually varying bottom topography, we employ the mild slope wave equation to describe its motion. Denote the water surface elevation caused by the wave motion by $\tilde{\eta} = \eta(x, y)e^{-i\sigma t}$, where σ is the angular frequency and $\eta(x, y)$ is called the complex amplitude of the component wave (the modulus of η denotes the usual wave amplitude and the argument of η represents the relative phase of the water surface elevation). The governing equation for η can then be written as (Berkhoff, 1972)

$$\nabla \cdot (CC_{\mathrm{g}}\nabla\eta) + k^2CC_{\mathrm{g}}\eta = 0 \tag{1}$$

where ∇ is the horizontal gradient operator, k the wavenumber, C the wave celerity and C_{g} the group velocity. Eq. (1) is for waves without any dissipation. If the dissipation effect is not negligible, we may have to introduce a factor $\mu = 1 + i\xi$ in the equation so that

$$\nabla \cdot (CC_{\mathrm{g}}\nabla\eta) + \mu^2k^2CC_{\mathrm{g}}\eta = 0 \tag{2}$$

Eq. (2) is slightly different from a previous equation proposed by Dalrymple et al. (1984). It is expected that the parameter ξ, that is, the imaginary part of the factor μ, can be more closely related to the conventional energy decaying factor

Φ_D (see, *e.g.*, Horikawa, 1989) so that the dissipation effect can be readily evaluated. The relation between ξ and Φ_D is clear if we consider a progressive wave in the positive x direction over a constant water depth. Under this circumstance, the energy decaying factor Φ_D is

$$\Phi_D = -\frac{1}{EC_g}\frac{d(EC_g)}{dx} = -\frac{1}{E}\frac{dE}{dx} \tag{3}$$

since C_g, which depends on the wave frequency and the water depth, is constant. E in (3) is the average wave energy, which can be expressed by

$$E = \frac{1}{8}\rho g H^2 \tag{4}$$

for small amplitude waves, where H is the wave height, ρ the fluid density and g the gravitational acceleration. Inserting (4) into (3) gives

$$\Phi_D = -\frac{2}{H}\frac{dH}{dx} \tag{5}$$

On the other hand, for a unidirectional wave, Eq. (2) reduces to

$$\frac{d^2\eta}{dx^2} + \mu^2 k^2 \eta = 0 \tag{6}$$

Eq. (6) has two independent solutions, representing the progressive decaying waves in the positive and negative x directions, respectively. The wave in the positive x direction can be expressed by

$$\eta = \eta|_{x_0} e^{-\xi k(x-x_0)} e^{ik(x-x_0)} \tag{7}$$

where x_0 denotes a reference point. Eq. (7) gives the variation of the wave height H as follows:

$$H = H|_{x_0} e^{-\xi k(x-x_0)} \tag{8}$$

Inserting (8) into (5), we readily obtain

$$\xi = \frac{1}{2k}\Phi_D \tag{9}$$

Perturbation of the Basic Equation

We introduce a principal angular frequency and denote it by $\bar{\sigma}$. $\bar{\sigma}$ may, but not necessarily, be defined as the peak angular frequency of the incident wave spectrum. With the principal angular frequency, the angular frequency σ of any component wave can be expressed as

$$\sigma = \bar{\sigma}(1+\epsilon) \tag{10}$$

where $\epsilon = (\sigma - \bar{\sigma})/\bar{\sigma}$. As long as we consider only narrow-banded waves, ϵ is a small quantity and all the frequency dependent variables may then be expanded into power series of ϵ at their principal values. In particular, for the surface elevation η, the wavenumber k and the product of the wave celerity C with the group velocity C_g, we have the following perturbation expressions:

$$\eta = \eta^{(0)} + \epsilon\eta^{(1)} + \epsilon^2\eta^{(2)} + \cdots \tag{11}$$

$$k = \bar{k}(1 + \epsilon\alpha^{(1)} + \epsilon^2\alpha^{(2)} + \cdots) \tag{12}$$

$$CC_g = \bar{C}\bar{C}_g(1 + \epsilon\beta^{(1)} + \epsilon^2\beta^{(2)} + \cdots) \tag{13}$$

where

$$\alpha^{(1)} = \frac{\bar{\sigma}}{\bar{k}}\overline{\frac{dk}{d\sigma}} = \frac{1}{\bar{n}} \tag{14}$$

$$\alpha^{(2)} = \frac{1}{2}\frac{\bar{\sigma}^2}{\bar{k}}\overline{\frac{d^2k}{d\sigma^2}} = -\frac{1}{2\bar{n}^3}[(2\bar{n}-1)\bar{m} - \bar{n}^2] \tag{15}$$

$$\beta^{(1)} = \frac{\bar{\sigma}}{\overline{CC_g}}\overline{\frac{dCC_g}{d\sigma}} = \frac{1}{\bar{n}^2}[(2\bar{n}-1)\bar{m} - \bar{n}] \tag{16}$$

$$\begin{aligned}\beta^{(2)} &= \frac{1}{2}\frac{\bar{\sigma}^2}{\overline{CC_g}}\overline{\frac{d^2CC_g}{d\sigma^2}} \\ &= \frac{1}{2\bar{n}^4}[(2\bar{n}-1)\bar{m}^2 + 3\bar{n}(\bar{n}-1)(2\bar{n}-1)\bar{m} - \bar{n}^2(5\bar{n}-4)]\end{aligned} \tag{17}$$

and

$$\bar{n} = \frac{1}{2}\left(1 + \frac{2\bar{k}h}{\sinh 2\bar{k}h}\right) \tag{18}$$

$$\bar{m} = \bar{n} + \frac{1}{2}\left(1 - \frac{2\bar{k}h}{\tanh 2\bar{k}h}\right) \tag{19}$$

The bars are used to denote principal values. It is obvious that $\alpha^{(1)}$, $\alpha^{(2)}$, $\beta^{(1)}$ and $\beta^{(2)}$ are all single functions of $\bar{k}h$ and, consequently, the principal wave effect parameter $\bar{\sigma}^2h/g$ if the following dispersion relation for the principal wave is taken into consideration:

$$\frac{\bar{\sigma}^2 h}{g} = \bar{k}h \tanh \bar{k}h \tag{20}$$

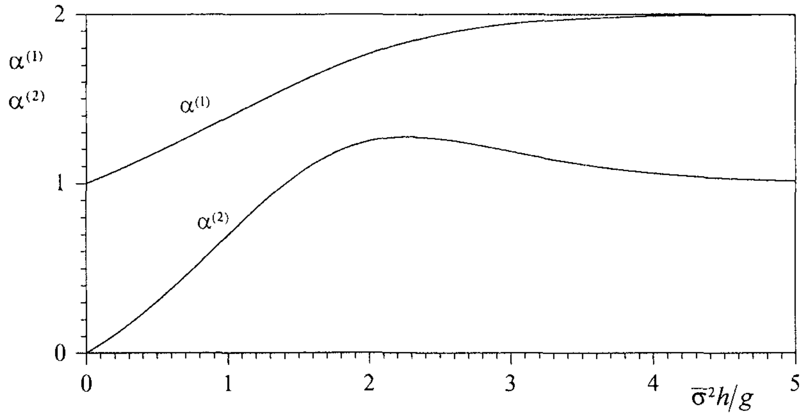

Fig. 1: Variation of $\alpha^{(1)}$ and $\alpha^{(2)}$ versus $\bar{\sigma}^2 h/g$

In **Figs. 1** and **2** we show these functional relations for $0 \leq \bar{\sigma}^2 h/g \leq 5$. It can be noted that when the principal wave tends to be a long wave, that is, $\bar{\sigma}^2 h/g$ tends to zero, $\alpha^{(1)}$ tends to 1 while $\alpha^{(2)}$, $\beta^{(1)}$ and $\beta^{(2)}$ all tend to zero. On the other hand, when the principal wave becomes a deep water wave, or, when $\bar{\sigma}^2 h/g$ tends to infinity, $\alpha^{(1)}$ tends to 2, $\alpha^{(2)}$ tends to 1, $\beta^{(1)}$ tends to -2 and $\beta^{(2)}$ tends to 3.

Substituting (11), (12) and (13) into the mild slope wave equation (2) and collecting all the terms for each order of ϵ, we obtain

$$\nabla \cdot (\bar{C}\bar{C}_g \nabla \eta^{(0)}) + \mu^2 \bar{k}^2 \bar{C}\bar{C}_g \eta^{(0)} = 0 \tag{21}$$

$$\nabla \cdot \left[\bar{C}\bar{C}_g \nabla \eta^{(1)} + \beta^{(1)} \bar{C}\bar{C}_g \nabla \eta^{(0)}\right] + \mu^2 \bar{k}^2 \bar{C}\bar{C}_g \left[\eta^{(1)} + \beta^{(1)} \eta^{(0)} + 2\alpha^{(1)} \eta^{(0)}\right] = 0 \tag{22}$$

$$\begin{aligned} \nabla \cdot \left[\bar{C}\bar{C}_g \nabla \eta^{(2)} + \beta^{(1)} \bar{C}\bar{C}_g \nabla \eta^{(1)} + \beta^{(2)} \bar{C}\bar{C}_g \nabla \eta^{(0)}\right] + \mu^2 \bar{k}^2 \bar{C}\bar{C}_g \Big[\eta^{(2)} + \beta^{(1)} \eta^{(1)} \\ + 2\alpha^{(1)} \eta^{(1)} + \beta^{(2)} \eta^{(0)} + 2\beta^{(1)} \alpha^{(1)} \eta^{(0)} + {\alpha^{(1)}}^2 \eta^{(0)} + 2\alpha^{(2)} \eta^{(0)}\Big] = 0 \end{aligned} \tag{23}$$

$$\cdots\cdots$$

where μ is treated as frequency independent. By considering (21) in (22) and, (21) and (22) in (23), Eqs. (22) and (23) may be simplified to give

$$\nabla \cdot (\bar{C}\bar{C}_g \nabla \eta^{(1)}) + \mu^2 \bar{k}^2 \bar{C}\bar{C}_g \eta^{(1)} + \bar{C}\bar{C}_g \nabla \beta^{(1)} \cdot \nabla \eta^{(0)} + 2\mu^2 \bar{k}^2 \bar{C}\bar{C}_g \alpha^{(1)} \eta^{(0)} = 0 \tag{24}$$

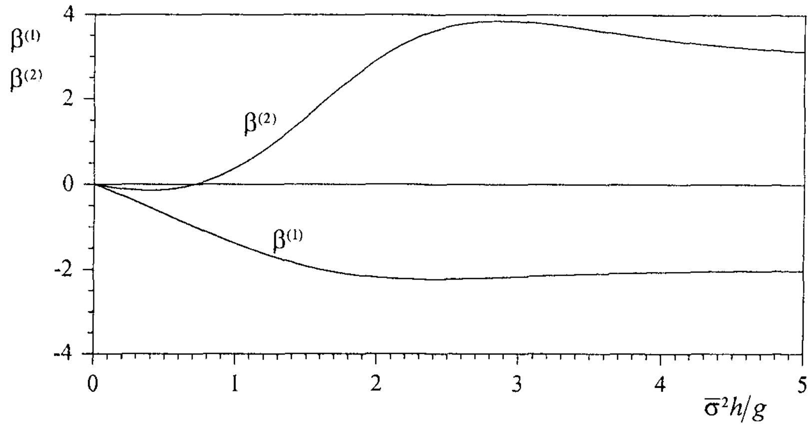

Fig. 2: Variation of $\beta^{(1)}$ and $\beta^{(2)}$ versus $\bar{\sigma}^2 h/g$

$$\nabla \cdot (\bar{C}\bar{C}_g \nabla \eta^{(2)}) + \mu^2 \bar{k}^2 \bar{C}\bar{C}_g \eta^{(2)} + \bar{C}\bar{C}_g \left[\nabla \beta^{(1)} \cdot \nabla \eta^{(1)} - \beta^{(1)} \nabla \beta^{(1)} \cdot \nabla \eta^{(0)} \right.$$
$$\left. + \nabla \beta^{(2)} \cdot \nabla \eta^{(0)} \right] + 2\mu^2 \bar{k}^2 \bar{C}\bar{C}_g \left[2\alpha^{(1)} \eta^{(1)} + \alpha^{(1)} \alpha^{(1)} \eta^{(0)} + 2\alpha^{(2)} \eta^{(0)} \right] = 0 \tag{25}$$

Eqs. (21), (24) and (25) may be used to solve $\eta^{(0)}$, $\eta^{(1)}$, $\eta^{(2)}$ and, therefore, η approximately. It is obvious that the zeroth order equation (21) describes the motion of the principal wave. This implies that the representative wave method is the leading order approximation of the present approach. Eqs. (24) and (25) govern the higher order modifications. The higher order equations all include a source term which depends on the lower order solutions. We also note that the equations for all orders can be expressed in a unified form as follows:

$$\nabla \cdot (\bar{C}\bar{C}_g \nabla \eta^{(m)}) + \mu^2 \bar{k}^2 \bar{C}\bar{C}_g \eta^{(m)} + q^{(m)} = 0 \qquad (m = 0, 1, 2, \cdots) \tag{26}$$

where

$$q^{(0)} = 0 \tag{27}$$

$$q^{(1)} = \bar{C}\bar{C}_g \nabla \beta^{(1)} \cdot \nabla \eta^{(0)} + 2\mu^2 \bar{k}^2 \bar{C}\bar{C}_g \alpha^{(1)} \eta^{(0)} \tag{28}$$

$$q^{(2)} = \bar{C}\bar{C}_g \left[\nabla \beta^{(1)} \cdot \nabla \eta^{(1)} - \beta^{(1)} \nabla \beta^{(1)} \cdot \nabla \eta^{(0)} + \nabla \beta^{(2)} \cdot \nabla \eta^{(0)} \right]$$
$$+ 2\mu^2 \bar{k}^2 \bar{C}\bar{C}_g \left[2\alpha^{(1)} \eta^{(1)} + \alpha^{(1)} \alpha^{(1)} \eta^{(0)} + 2\alpha^{(2)} \eta^{(0)} \right] \tag{29}$$

......

Boundary Conditions

We consider two kinds of boundaries. The first kind is where the free surface oscillation is given by

$$\eta = ae^{i\theta} \tag{30}$$

where a is the amplitude and θ the phase. For each order, we require

$$\eta^{(0)} = ae^{i\theta} \tag{31}$$

$$\eta^{(m)} = 0 \qquad (m \geq 1) \tag{32}$$

The second kind of boundary condition is assumed to be expressed in the following form:

$$\frac{\partial \eta}{\partial n} - i\lambda k\eta + i\nu k = 0 \tag{33}$$

where λ and ν are constants related to the physical situation (Yu et al., 1992). In particular, an impermeable boundary is represented by $\lambda = 0$ and $\nu = 0$.

Substituting (11) and (12) into (33) and collecting all the terms for each order of ϵ, we obtain

$$\frac{\partial \eta^{(0)}}{\partial n} - i\lambda\bar{k}\eta^{(0)} + i\nu\bar{k} = 0 \tag{34}$$

$$\frac{\partial \eta^{(1)}}{\partial n} - i\lambda\bar{k}\eta^{(1)} - i\lambda\alpha^{(1)}\bar{k}\eta^{(0)} + i\nu\alpha^{(1)}\bar{k} = 0 \tag{35}$$

$$\frac{\partial \eta^{(2)}}{\partial n} - i\lambda\bar{k}\eta^{(2)} - i\lambda\bar{k}(\alpha^{(1)}\eta^{(1)} + \alpha^{(2)}\eta^{(0)}) + i\nu\alpha^{(2)}\bar{k} = 0 \tag{36}$$

$$\cdots\cdots$$

The above equations have the following unified form:

$$\frac{\partial \eta^{(m)}}{\partial n} - i\lambda\bar{k}\eta^{(m)} + p^{(m)} = 0 \qquad (m = 0, 1, 2, \cdots) \tag{37}$$

where

$$p^{(0)} = i\nu\bar{k} \tag{38}$$

$$p^{(1)} = -i\lambda\alpha^{(1)}\bar{k}\eta^{(0)} + i\nu\alpha^{(1)}\bar{k} \tag{39}$$

$$p^{(2)} = -i\lambda\bar{k}(\alpha^{(1)}\eta^{(1)} + \alpha^{(2)}\eta^{(0)}) + i\nu\alpha^{(2)}\bar{k} = 0 \tag{40}$$

$$\cdots\cdots \tag{41}$$

FINITE ELEMENT METHOD

It is known that the solution of the elliptic equation (26) when subjected to the boundary condition (37) stagnates the following functional in terms of $\eta^{(m)}$:

$$\Pi = \int_{\Omega}\left[\frac{1}{2}\bar{C}\bar{C}_{\mathrm{g}}\nabla\eta^{(m)}\cdot\nabla\eta^{(m)} - \frac{1}{2}\mu^2\bar{k}^2\bar{C}\bar{C}_{\mathrm{g}}\eta^{(m)}\eta^{(m)} - q^{(m)}\eta^{(m)}\right]d\Omega \\ + \int_{\Gamma_2}\left[-\frac{1}{2}i\lambda\bar{k}\bar{C}\bar{C}_{\mathrm{g}}\eta^{(m)}\eta^{(m)} + p^{(m)}\eta^{(m)}\right]d\Gamma \tag{42}$$

where Ω is the domain of interest and Γ_2 the part of the boundary of Ω where (37) must be satisfied. For a finite element solution of $\eta^{(m)}$ which stagnates Π in some approximate sense, we discretize the domain Ω into elements and let all the elements be related to each other through the nodes located on the common boundaries of the elements. Denote

$$\Pi^e = \int_{\Omega^e}\left[\frac{1}{2}\bar{C}\bar{C}_{\mathrm{g}}\nabla\eta^{(m)}\cdot\nabla\eta^{(m)} - \frac{1}{2}\mu^2\bar{k}^2\bar{C}\bar{C}_{\mathrm{g}}\eta^{(m)}\eta^{(m)} - q^{(m)}\eta^{(m)}\right]d\Omega \\ + \int_{\Gamma^e}\left[-\frac{1}{2}i\lambda\bar{k}\bar{C}\bar{C}_{\mathrm{g}}\eta^{(m)}\eta^{(m)} + p^{(m)}\eta^{(m)}\right]d\Gamma \tag{43}$$

where Ω^e is an element and Γ^e its boundary, $\lambda = 0$ and $\nu = 0$ if $\Gamma^e \notin \Gamma_2$. Eq. (42) can then be written as

$$\Pi = \sum_e \Pi^e \tag{44}$$

We introduce the primed indices $1', 2', \cdots, N'$ in the anti-clockwise fashion in each element for locally numbering the nodes related to the element and assume the global nodal numbers of $1', 2', \cdots, N'$ to be $n^e_{1'}, n^e_{2'}, \cdots, n^e_{N'}$, respectively. As interpolation functions $L^e_{i'}(x, y)$ $(i' = 1', 2', \cdots, N')$ are defined in each element, any function $F(x, y)$ in Ω^e can be approximated in terms of its nodal values $F_{1'}$, $F_{2'}$, $\cdots$, $F_{N'}$ as

$$F(x, y) = L^e_{i'}F_{i'} \tag{45}$$

where the summation convention is implicit. Therefore, Π^e can be partially evaluated so as to give

$$\Pi^e = \frac{1}{2}K^e_{i'j'}\eta^{(m)}_{i'}\eta^{(m)}_{j'} + f^{(m)e}_{j'}\eta^{(m)}_{j'} \tag{46}$$

where $K^e_{i'j'}$ is a $N' \times N'$ matrix depending on the interpolation functions as well as the local features of the principal wave. With the following matrix

$$T^e_{i'i} = \begin{cases} 1 & \text{when} \quad n_{i'} = i \\ 0 & \text{when} \quad n_{i'} \neq i \end{cases} \quad (i' = 1', 2', \cdots, N' \text{ and } i = 1, 2, \cdots N) \tag{47}$$

where N is the total number of nodes, we have

$$\eta_{i'}^{(m)} = T_{i'i}^e \eta_i^{(m)} \tag{48}$$

Eq. (46) can then be expressed by

$$\Pi^e = \frac{1}{2}\left(K_{i'j'}^e T_{i'i}^e T_{j'j}^e\right)\eta_i^{(m)}\eta_j^{(m)} + \left(f_{j'}^{(m)e} T_{j'j}^e\right)\eta_j^{(m)} \tag{49}$$

Therefore,

$$\Pi = \frac{1}{2}\left(\sum_e K_{i'j'}^e T_{i'i}^e T_{j'j}^e\right)\eta_i^{(m)}\eta_j^{(m)} + \left(\sum_e f_{j'}^{(m)e} T_{j'j}^e\right)\eta_j^{(m)} \tag{50}$$

$$= \frac{1}{2} K_{ij}\eta_i^{(m)}\eta_j^{(m)} + F_j^{(m)}\eta_j^{(m)} \tag{51}$$

where

$$K_{ij} = \sum_e K_{i'j'}^e T_{i'i}^e T_{j'j}^e \qquad \text{and} \qquad F_j^{(m)} = \sum_e f_{j'}^{(m)e} T_{j'j}^e \tag{52}$$

From the necessary condition for Π to be stagnated:

$$\frac{\delta \Pi}{\delta \eta_j^{(m)}} = 0 \tag{53}$$

we obtain the following linear algebraic equations:

$$K_{ij}\eta_i^{(m)} + F_j^{(m)} = 0 \tag{54}$$

since the matrix K_{ij} is symmetric. When modified so that the forced boundary condition is satisfied, Eq. (54) gives the nodal values of $\eta^{(m)}$. It may be noted that the matrix K_{ij} is independent of the order of perturbation. This implies that, if the LU decomposition method is utilized to solve the finite element equations, we need to carry out the decomposition only once for solving all the perturbation equations. The computational efforts involved in our numerical model are, therefore, equivalent to those required by the representative wave method.

WAVE MOTION OVER AN ELLIPTIC SHOAL

We apply our numerical model to the study of the unidirectional and narrow-banded irregular wave transformation over an elliptic shoal, a problem which has been investigated by Vincent and Briggs (1989) and by Panchang et al. (1990) with different methods. The topography and the incident wave conditions in our study are made identical to the U4 case of Vincent and Briggs (1989) and Panchang et al. (1990) so that our numerical results may be verified. The computational domain is sketched in **Fig. 3**, where the shoal is centered at $x = 0$ and $y = 0$ and the perimeter of the shoal is described by

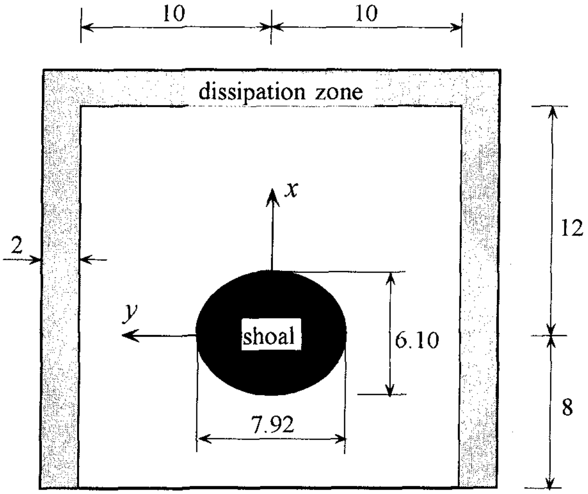

Fig. 3: The computational domain (all numbers are measured in meters)

$$\left(\frac{x}{3.05}\right)^2 + \left(\frac{y}{3.96}\right)^2 = 1 \tag{55}$$

The water depth is

$$h(x,y) = 0.9144 - 0.7620\left\{1 - \left(\frac{x}{3.81}\right)^2 - \left(\frac{y}{4.95}\right)^2\right\}^{\frac{1}{2}} \qquad \text{(m)} \tag{56}$$

over the shoal and is 0.4572m in the rest of the domain.

The incident wave is assumed to have the following σ-spectrum:

$$S(\sigma) = \phi\psi g^2\sigma \exp\left\{-1.25\left(\frac{\bar{\sigma}}{\sigma}\right)^4 + \ln\gamma \exp\left[-\frac{(\sigma-\bar{\sigma})^2}{2\chi\bar{\sigma}^2}\right]\right\} \tag{57}$$

where S is so defined that the energy associated with the component waves of the angular frequency between σ and $\sigma + \Delta\sigma$ is $E = \rho g S(\sigma)\Delta\sigma$; the depth-effect parameter ϕ is evaluated through

$$\phi = \begin{cases} 0.5\nu^2 & \text{for } \nu < 1 \\ 1 - 0.5(2-\nu)^2 & \text{for } 1 \le \nu \le 2 \\ 1 & \text{for } \nu > 2 \end{cases} \tag{58}$$

where $\nu = \sigma(h/g)^{1/2}$; the shape factor χ is

$$\chi = \begin{cases} 0.07 & \text{for } \sigma < \bar{\sigma} \\ 0.09 & \text{for } \sigma \ge \bar{\sigma} \end{cases} \tag{59}$$

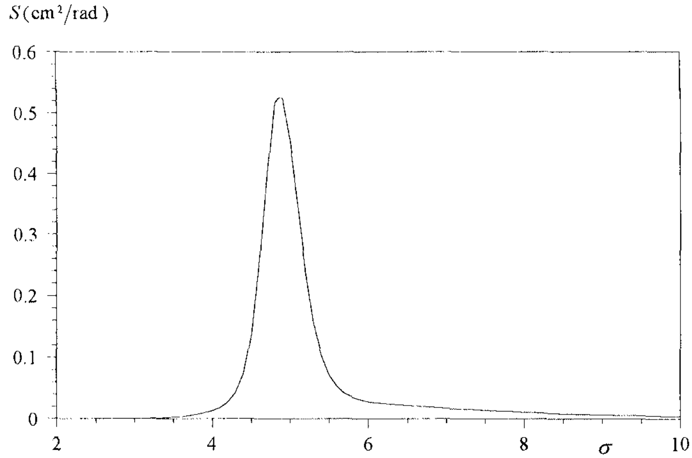

Fig. 4: The incident wave spectrum

γ is the peak enhancement factor and ψ the Phillips constant. For the present case where $\gamma = 20$, $\psi = 0.00047$ and the peak angular frequency $\bar{\sigma} = 4.833$, the spectrum is demonstrated in **Fig. 4**. As it can be noted, most of the incident wave energy is banded between $\sigma = 4$ and 6. It is then reasonable to represent the spectral incident wave by the superposition of the component waves with the following discrete angular frequencies:

$$\sigma_n = 4.0 + n\Delta\sigma \qquad (n = 0, 1, \cdots, 50) \tag{60}$$

where $\Delta\sigma = 0.04$. Following Longuet-Higgins (1957) we have

$$\tilde{\eta} = \sum_{n=0}^{50} a_n e^{i\theta_n} e^{i\sigma_n t} \tag{61}$$

where $a_n = \sqrt{2S(\sigma_n)\Delta\sigma}$ is the amplitude of the nth component wave and θ_n are random values with a uniform distribution between 0 and 2π. The forced boundary condition for the nth component wave in our problem can then be specified as

$$\eta = a_n e^{i\theta_n} \tag{62}$$

The lateral and downwave boundaries in our problem should be totally transmissive, that is, the boundary conditions should be specified so that the outgoing waves are totally absorbed by the boundaries. This requirement can be approximately met through the following numerical installation. We place a two-meter

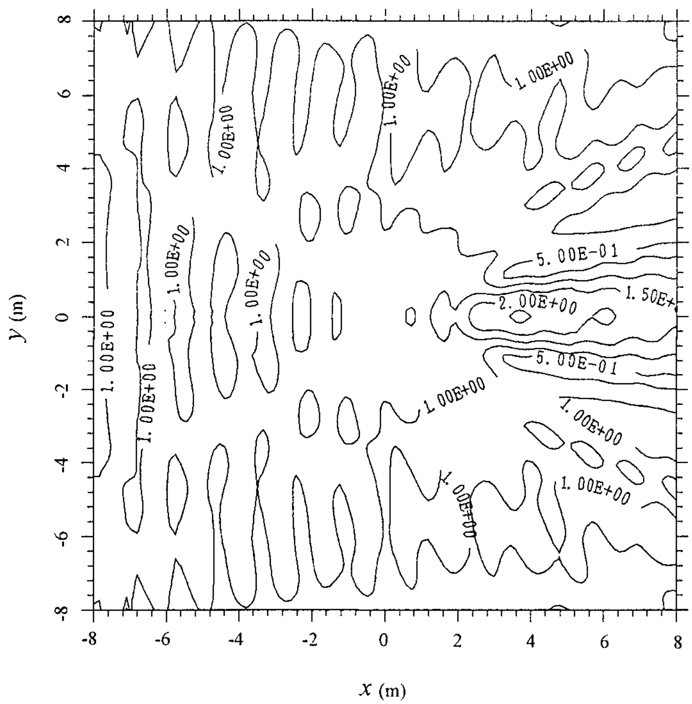

Fig. 5: Computed wave height distribution

dissipative layer with $\mu = 1 + 0.5i$ along the transmissive boundaries. The function of the dissipative layer is as same as the wave absorber in a physical model. The artificial boundaries at $y = \pm 12$m are assumed to be impermeable and, therefore, the boundary conditions there are expressed by (33) with $\lambda = 0$ and $\nu = 0$. The boundary at $x = 14$m is required to be non-reflective to the principal wave. The boundary condition can then be expressed by (33) with $\lambda = 1$ and $\nu = 0$.

In the computation, the domain is discretized into triangular elements with a dimension equivalent to one-fifteenth of the principal wavelength over the flat bottom. Linear interpolation functions are employed. **Fig. 5** shows the resulted distribution of the significant wave height (normalized by the significant incident wave height H_0). In **Fig. 6** we compare the computed wave height, at $x = 2.28m$, with the experimental data obtained by Vincent and Briggs (1989) and by Panchang et al. (1990). The agreement between the numerical solution

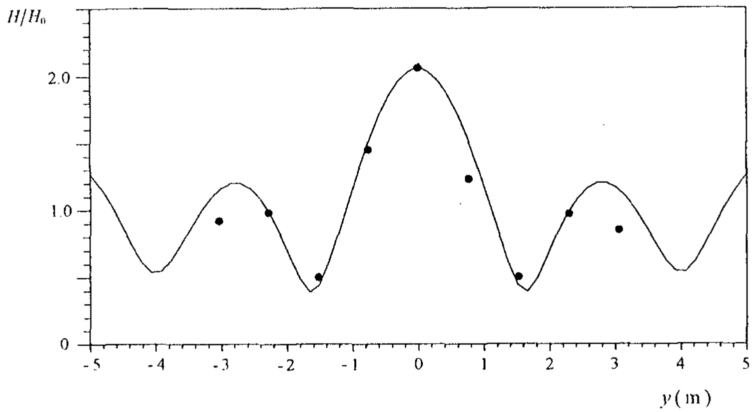

Fig. 6: Comparison of the computed wave height with experimental data

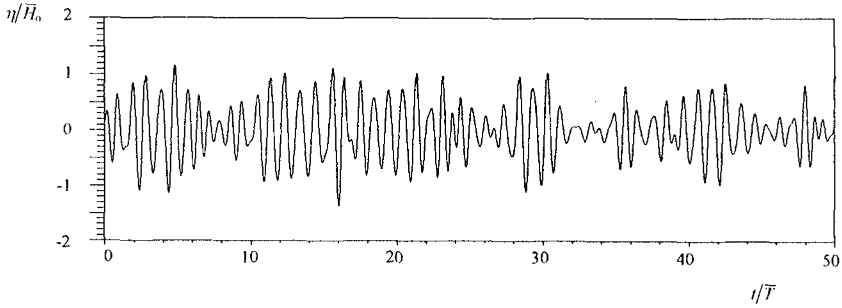

Fig. 7: Water surface elevation over the top of the shoal

and laboratory measurement is shown fairly satisfactory. In **Fig. 7** we plot the assembled irregular wave profile (normalized by the mean incident wave height $\bar{H}_0$) over the top of the shoal.

CONCLUSIONS

We presented a numerical model for the analysis of narrow-banded irregular wave transformation over gradually varying bottom topography. The model is based on the mild slope wave equation for component waves. By regular perturbation, the mild slope wave equation, which depends on the frequency of the component wave, leads to the perturbation equations in terms of the principal wave parameters. The finite element method has been suggested for numerical solutions of the perturbation equations. Since the matrix of the linear algebraic finite element equations depends on neither the component wave properties nor the order of the perturbation, the computational efforts involved in the present model is equivalent to those required by the representative wave method. The model has been applied to the computation of the wave motion over an elliptic shoal. Satisfactory agreement between the numerical solution and experimental data has been obtained.

REFERENCES

Berkhoff, J. W. C. (1972). Computation of combined refraction-diffraction. *Proc. 13th Conf. on Coast. Engrg.*, 471–490.

Dalrymple, R. A., Kirby, J. T. and Hwang, P. A. (1984). Wave diffraction due to areas of energy dissipation, *J. Wtrwy., Port, Coast. and Oc. Engrg.*, ASCE, 110(1), 67–79.

Goda, Y. (1985). *Random Seas and Design of Maritime Structures.* University of Tokyo Press, 323p.

Horikawa, K. (1989). *Nearshore Dynamics and Coastal Processes—Theory, Measurement and Predictive Model*, University of Tokyo Press, 522p.

Karlsson, T. (1969). Refraction of continuous ocean wave spectra, *Proc. Amer. Soc. Civ. Engrs.*, 95(WW4), 437-448.

Longuet-Higgins, M. S. (1957). The statistical analysis of a random, moving surface, *Phil. Trans. Roy. Soc. London*, 249(A), 321-387.

Panchang V. G., Wei, G., Pearce, B. R. and Briggs, M. J. (1990). Numerical simulation of irregular waves propagation over shoal, *J. Wtrwy., Port, Coast. and Oc. Engrg.*, ASCE, 116(3), 324–340.

Vincent, C. L. and Briggs, M. J. (1989). Refraction and diffraction of irregular waves over a mound. *J. Wtrwy., Port, Coast. and Oc. Engrg.*, ASCE, 115(2), 269–284.

Yu, X., Isobe, M. and Watanabe, A. (1992). Finite element solution of wave field around structures in nearshore zone, *Cost. Engrg. in Japan*, JSCE, 35(1), 21-33.